

HOSTED BY



ELSEVIER

Contents lists available at ScienceDirect

## Journal of Pharmacological Sciences

journal homepage: [www.elsevier.com/locate/jphs](http://www.elsevier.com/locate/jphs)

Full paper

## Myeloid HIF-1 attenuates the progression of renal fibrosis in murine obstructive nephropathy

Yu Tateishi <sup>a, b, c</sup>, Mayuko Osada-Oka <sup>e</sup>, Masako Tanaka <sup>a</sup>, Masayuki Shiota <sup>d</sup>, Yasukatsu Izumi <sup>d</sup>, Eiji Ishimura <sup>b</sup>, Koka Motoyama <sup>c</sup>, Masaaki Inaba <sup>c</sup>, Katsuyuki Miura <sup>a, \*</sup><sup>a</sup> Department of Applied Pharmacology and Therapeutics, Osaka City University Medical School, Asahimachi, Abeno-ku, Osaka 545-8585, Japan<sup>b</sup> Department of Nephrology, Osaka City University Medical School, Asahimachi, Abeno-ku, Osaka 545-8585, Japan<sup>c</sup> Department of Metabolism, Endocrinology and Molecular Medicine, Osaka City University Medical School, Asahimachi, Abeno-ku, Osaka 545-8585, Japan<sup>d</sup> Department of Pharmacology, Osaka City University Medical School, Asahimachi, Abeno-ku, Osaka 545-8585, Japan<sup>e</sup> Food Hygiene and Environmental Health Division of Applied Life Science, Graduate School of Life and Environmental Sciences, Kyoto Prefectural University, Sakyo-ku, Kyoto 606-8522, Japan

## ARTICLE INFO

## Article history:

Received 25 August 2014

Received in revised form

18 November 2014

Accepted 7 December 2014

Available online 27 December 2014

## Keywords:

Hypoxia-inducible factor

Renal fibrosis

Macrophage

## ABSTRACT

Hypoxia-inducible factors (HIFs) play an important role in the pathogenesis of renal fibrosis. Although the role of macrophage infiltration in the progression of renal fibrosis is well known, the role of macrophage HIF-1 remains to be revealed. To address this question, myeloid specific conditional HIF-1 knock out mice were subjected to unilateral ureteral obstruction (UUO). Renal interstitial deposition of collagen III and mRNA expressions of collagen I and collagen III were markedly increased at 7 days after UUO and myeloid HIF-1 depletion significantly accelerated these increases. Immunohistochemistry and flow cytometric analysis revealed that renal infiltrating macrophages were increased with duration of UUO but myeloid HIF-1 depletion did not affect these changes. Myeloid HIF-1 depletion did not affect M1 and M2 macrophage phenotype polarization in obstructed kidneys. Renal connective tissue growth factor (CTGF) expression was markedly increased and myeloid HIF-1 depletion further enhanced this increase. Immunomagnetic separation of renal cells revealed that renal CTGF was expressed predominantly in renal cells other than macrophages. It is suggested that myeloid HIF-1 attenuates the progression of renal fibrosis in murine obstructive kidney. Alteration of CTGF expression in renal cells other than macrophages is one of possible mechanisms by which myeloid HIF-1 protected renal fibrosis.

© 2015 Japanese Pharmacological Society. Production and hosting by Elsevier B.V. All rights reserved.

## 1. Introduction

Chronic kidney disease (CKD) is pathologically defined by the progression of tubulointerstitial fibrosis and glomerulosclerosis regardless of its cause (1). Although approximately 20% of total cardiac output circulates through the normal kidney, renal tissue is exposed to hypoxia (2). In CKD, this hypoxia becomes worse with exacerbation of renal injury (2).

Hypoxia-inducible factors (HIFs) are transcriptional factors that mediate cellular adaptation to hypoxia. HIF consists of oxygen-sensitive  $\alpha$  subunit and constitutively expressed  $\beta$  subunit. Under normoxic conditions, two proline residues of HIF- $\alpha$  are hydroxylated by oxygen-dependent HIF prolyl-4-hydroxylase domain enzyme

(PHD) that permit binding to ubiquitin ligase Von-Hippel-Lindau protein (pVHL) and subsequently degraded by proteasome. HIF- $\alpha$  is stabilized under hypoxic environment due to reduced activity of PHD and gets transcriptional activity via heterodimerization with  $\beta$  subunit (3). HIF- $\alpha$  consists of three isoforms including HIF-1 $\alpha$ , HIF-2 $\alpha$ , and HIF-3 $\alpha$ . Within the kidney, HIF-1 $\alpha$  is expressed in many types of cells, but HIF-2 $\alpha$  expression is much restricted. Little is known about HIF-3 $\alpha$  expression and its role (4).

Pharmacological activation of HIF by PHD inhibition attenuated acute and chronic kidney injury (5, 6). In contrast, other groups reported that renal tubular HIF-1 promotes tubulointerstitial injury (7, 8). Renal tissue is composed of various cell types and the distribution of each HIF isoform is heterogeneous. Therefore, it is important to clarify the role of individual HIF isoform in each cell population in the pathophysiology of kidney diseases.

We and other group previously reported that renal infiltrating macrophages promotes the development of renal fibrosis in murine

\* Corresponding author. Tel.: +81 6 6645 3787; fax: +81 6 6646 3048.

E-mail address: [miura-pha@med.osaka-cu.ac.jp](mailto:miura-pha@med.osaka-cu.ac.jp) (K. Miura).

Peer review under responsibility of Japanese Pharmacological Society.

unilateral ureteral obstruction (UUO) model (9–11). Myeloid HIF-1 $\alpha$  plays an important role in regulation of myeloid cell functions. HIF-1 $\alpha$  promotes phagocytosis (12) and macrophage polarization to M1 phenotype known as classically activated phenotype (13–15). However, the role of macrophage HIF-1 in the renal fibrogenesis remains to be elucidated. In this study, we elucidated the role of myeloid HIF-1 in the development of renal fibrosis by using mice with HIF-1 $\alpha$  depleted in myeloid cells.

## 2. Materials and methods

### 2.1. Animals

Myeloid cell-specific HIF-1 depleted mice on the C57BL/6J background (HIF-1 $\alpha^{\text{flox/flox}}$  LysM-Cre $+/+$ : HIFKO group) and control mice (HIF-1 $\alpha^{\text{flox/flox}}$  LysM-Cre $-/-$ : WT group) were obtained by crossing HIF-1 $\alpha^{\text{flox/flox}}$  mice with mice expressing Cre recombinase under the control by the Lysozyme M promoter (Jackson Laboratories, Bar Harbor, ME, USA). All procedures using mice were performed in accordance with Science Council of Japan Guideline for Proper Conduct of Animal Experiments and were approved by Osaka City University.

### 2.2. UUO model

UUO was performed aseptically as previously described (9, 10). At 3 or 7 days after UUO, kidneys were perfused with ice-cold saline via heart puncture and harvested under anesthesia.

### 2.3. Cell culture

To obtain bone marrow derived macrophages (BMDM), we collected bone marrow cells from mouse femurs and tibias. Cells were plated into bacteriological petri dish and cultured in DMEM containing 10% fetal bovine serum and 20% L929 conditioned media for 7 days. Adherent cells were collected by Cellstripper (Corning, Manassas, VA, USA), plated into culture dishes and used for experiments.

### 2.4. Immunoblotting analysis

In order to assess the expression of the HIF-1 $\alpha$  and HIF-2 $\alpha$  protein in BMDM and renal connective tissue growth factor (CTGF) proteins at 7 days after UUO, immunoblotting analysis was performed. Protein extracts obtained from BMDM (20  $\mu$ g) or kidneys at 7 days after UUO (30  $\mu$ g) were separated on SDS-polyacrylamide gels and transferred to PVDF membranes. Non-specific background was blocked by 2% skim milk in Tris-buffer saline containing 0.1% Tween-20 (TBS-T) at room temperature for 1 h, followed by incubation with rabbit anti-HIF-1 $\alpha$  antibody ( $\times$ 200, Cayman Chemical Co. Ann Arbor, MI, USA), rabbit anti-HIF-2 $\alpha$  antibody ( $\times$ 500, Novus Biologicals, Littleton, CO, USA) or rabbit anti-CTGF antibody ( $\times$ 250, Abcam, Cambridge, UK). Primary antibodies were detected using secondary antibodies conjugated with horseradish peroxidase. The membranes were detected with LAS-4000 lumino-image analyzer system (GE Healthcare Bio-Science, Piscataway, NJ, USA).

### 2.5. Immunohistochemistry

Kidneys were fixed with 4% paraformaldehyde and sections (4- $\mu$ m-thick) of the paraffin-embedded renal tissue were used for immunohistochemistry of Collagen III and F4/80 (+) mononuclear phagocytes as previously described (9, 10). Each microphotograph was digitized and the percentages of immunostained area of

Collagen III and F4/80 in the renal cortex were analyzed by using ImageJ 1.43 at a magnification of  $\times$ 200.

### 2.6. TUNEL assay

Apoptotic cells were detected by the terminal deoxynucleotidyl transferase (TdT)-mediated dUTP biotin nick end labeling assay using the In situ Apoptosis Detection Kit (Takara Bio Inc., Kyoto, Japan). TUNEL assay was performed for paraffin sections fixed with 4% paraformaldehyde and were processed according to manufacturer's manual. The number of TUNEL-positive tubular cells was counted in 10 cortical areas of each sample ( $\times$ 200).

### 2.7. Tubular injury score

Tubular injury was scored semiquantitatively in cortical areas of Periodic acid-Schiff (PAS) staining by the blinded observer. Tubular injury was defined as dilatation of tubular lumina, tubular atrophy, tubular cast formation, detachment of tubular epithelial cells, or thickening of tubular basement membrane. The score is that: 0, no tubular injury; 1, <10% of tubules injured; 2, 10–25% of tubules injured; 3, 26–50% of tubules injured; 4, 51–75% of tubules injured; 5, >75% of tubules injured.

### 2.8. Real-time reverse transcriptase-polymerase chain reaction (PCR)

Renal mRNA expression was determined by SYBR-green-based real-time reverse transcriptase PCR using a standard curve as previously reported (9, 10). The level of molecules investigated was corrected for 18S ribosomal RNA (18SrRNA) or hypoxanthine-guanine phosphoribosyltransferase (HPRT).

### 2.9. Preparation of kidney cell suspension for flow cytometry and separation by anti-CD11b antigen coupled magnetic beads (CD11b MACS beads)

Kidney cell suspension was prepared as previously described (9, 10). Briefly, kidneys were dissected, placed Hank's Balanced Salt Solution (HBSS) containing 1.6 mg/mL Collagenase IA (Sigma Aldrich, Tokyo, Japan) and 200  $\mu$ g/mL DNase I (Roche, Indianapolis, IN, USA) for 30 min at 37 °C with intermittent agitation and then washed twice in HBSS. Following erythrocyte lysis, cells were resuspended in FACS buffer (PBS/5% fetal calf serum/0.05% Na $_2$ ). Kidney cell suspensions were allowed to settle for 20 min after which the upper five-sixths were collected for use in flow cytometry. In some experiments, kidney cells were separated into CD11b (+) cells and CD11b (–) cells by CD11b MACS beads (Miltenyi Biotec, Auburn, CA, USA).

### 2.10. Flow cytometric analysis

Aliquots of cells were pre-incubated with anti-CD16/CD32 Fc receptor (2.4G2) (BD Bioscience, San Jose, CA, USA) for 15 min to minimize non-specific antibody binding. Cells were then incubated in FACS buffer at 4 °C with various combinations of fluorochrome-labeled antibodies. In order to stain infiltrating leukocytes, kidney cells were stained with antibody to CD45-PE/Cy7 (30-F11). Phycoerythrin (PE)-conjugated anti-mouse lineage antibody cocktail containing antibodies against CD90.2 (Thy1.2), B220 (RA3-6B2), CD49b (DX5), NK1.1 (PK136), Ly6G (1A8) was used (16). Renal infiltrating macrophages were defined as CD45 positive, lineage negative, CD11b positive (anti-CD11b-APC/Cy7, M1/70) cells. These macrophages were further grouped by the fluorescent intensity of surface expression of F4/80 (APC, BM8) and Ly6C (PerCP/Cy5.5,

HK1.4). All fluorochrome-labeled antibodies except for Ly6G (BD Bioscience, San Jose, CA, USA) were obtained from BioLegend (San Diego, CA, USA). Absolute cell counts of CD45 (+) cells and individual leukocyte subset number were determined by using fluorescent counting beads (TruCOUNT Tubes, BD Bioscience, San Jose, CA, USA).

### 2.11. Statistical analysis

All data are shown as the mean  $\pm$  S.E.M. Data were analyzed using ANOVA followed by Tukey's post hoc analysis or t-test where appropriate. As some data showed heteroscedasticity, logarithmic transformation was made before analysis. Statistical significance was defined as  $p < 0.05$ .

## 3. Results

### 3.1. Myeloid HIF-1 $\alpha$ expression was suppressed in LysM-Cre HIF-1 $\alpha^{lox/lox}$ mice

We evaluated HIF-1 $\alpha$  protein expression in BMDMs under normoxia (O<sub>2</sub> 21%) or hypoxia (O<sub>2</sub> 1%) for 24 h. Though macrophage HIF-1 $\alpha$  proteins were markedly increased by hypoxia in WT group, these increases were not observed in HIFKO group (Fig. 1A, B). As a reference, we also determined macrophage HIF-2 $\alpha$  protein expression. It was slightly increased by hypoxia and this increase reached statistically significant in WT group but not in HIFKO group. However, under hypoxic condition, no significant difference was observed between WT and HIFKO group (Fig. 1A, B). To estimate macrophage HIF-1 $\alpha$  mRNA expression in vivo, we collected CD11b (+) cells from kidney at 3 and 7 days after UUU by using CD11b MACS beads. HIF-1 $\alpha$  mRNA expression in HIFKO group was significantly lower than in WT group (Fig. 1C). We and another group reported that vast majority of renal CD11b (+) cells are macrophages and dendritic cells in murine obstructive kidney (10, 11). Therefore, these results indicate that HIF-1 $\alpha$  mRNA

expression in renal macrophages and dendritic cells was suppressed in HIFKO group.

### 3.2. Myeloid HIF-1 depletion promoted renal fibrosis in UUU

To evaluate the role of myeloid HIF-1 in the progression of renal fibrosis, we performed renal collagen III immunohistochemistry at 7 days after UUU. Renal collagen III deposition was markedly increased by UUU and myeloid HIF-1 depletion further enhanced the accumulation of collagen III (Fig. 2A, B). Furthermore, UUU markedly increased both renal collagen I and collagen III mRNA expressions and these increases were also significantly enhanced by myeloid HIF-1 depletion (Fig. 2C). These results suggest that myeloid HIF-1 depletion promoted the progression of renal fibrosis in UUU mice.

### 3.3. Myeloid HIF-1 depletion did not affect the renal macrophage accumulation in UUU

To examine the effects of myeloid HIF-1 depletion on renal macrophage infiltration, we performed immunohistochemistry of F4/80 positive cells (Fig. 3A, B). Renal F4/80 positive cells in the obstructed kidney were markedly increased with duration of UUU. However, genetic ablation of myeloid HIF-1 did not affect these increases. Similarly, myeloid HIF-1 depletion did not affect the increase in renal mRNA expression of EMR-1 (F4/80 antigen) seen in the obstructed kidney (Fig. 2C).

To characterize renal infiltrating macrophages in more detail, we performed flow cytometric analysis of kidney cell suspension at 3 and 7 days after UUU. Renal infiltrating macrophages were defined as CD45 (+), Lineage (-), CD11b (+) cells (16) (Fig. 3C). Again, cell number of renal infiltrating macrophages in the obstructed kidney were quantitatively same between WT and HIFKO group at 3 and 7 days after UUU (Fig. 3D).

Taken together, these results indicate that myeloid HIF-1 depletion did not affect the renal macrophage accumulation following UUU.

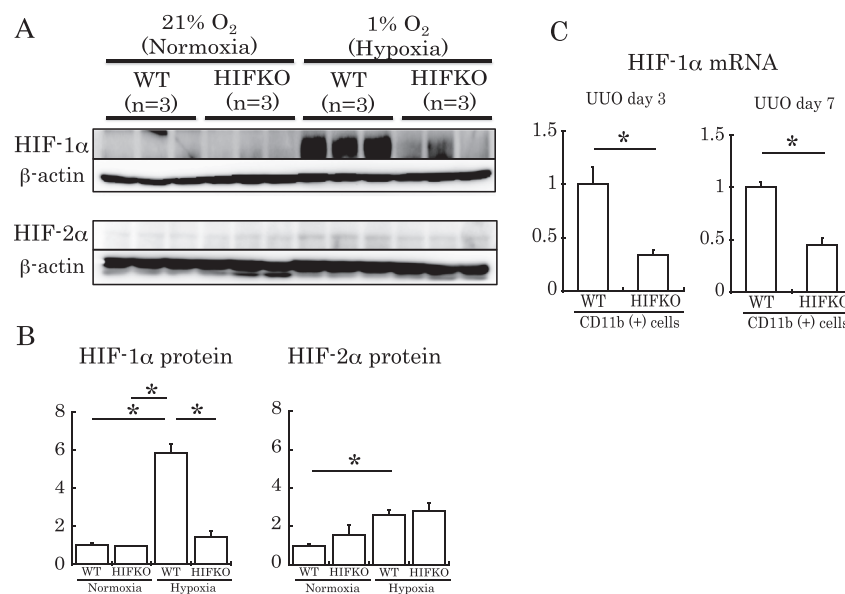


**Fig. 1.** HIF-1 $\alpha$  and HIF-2 $\alpha$  expression in myeloid cells. A) Immunoblotting of HIF-1 $\alpha$  and HIF-2 $\alpha$  proteins in BMDMs of WT and HIFKO mice incubated in normoxia (21% oxygen) and hypoxia (1% oxygen) for 24 h ( $n = 3$  in each group), and B) Quantitative evaluation of A). Each value was corrected for  $\beta$ -actin and protein expression of normoxic WT BMDMs was assigned to a unity. C) HIF-1 $\alpha$  mRNA expression in renal CD11b (+) cells which were separated by CD11b MACS beads at 3 and 7 days after UUU. Each value was corrected for HPRT and mRNA expression of WT CD11b (+) cells was assigned to a unity ( $n = 4-8$  in each group). \* $p < 0.05$ .

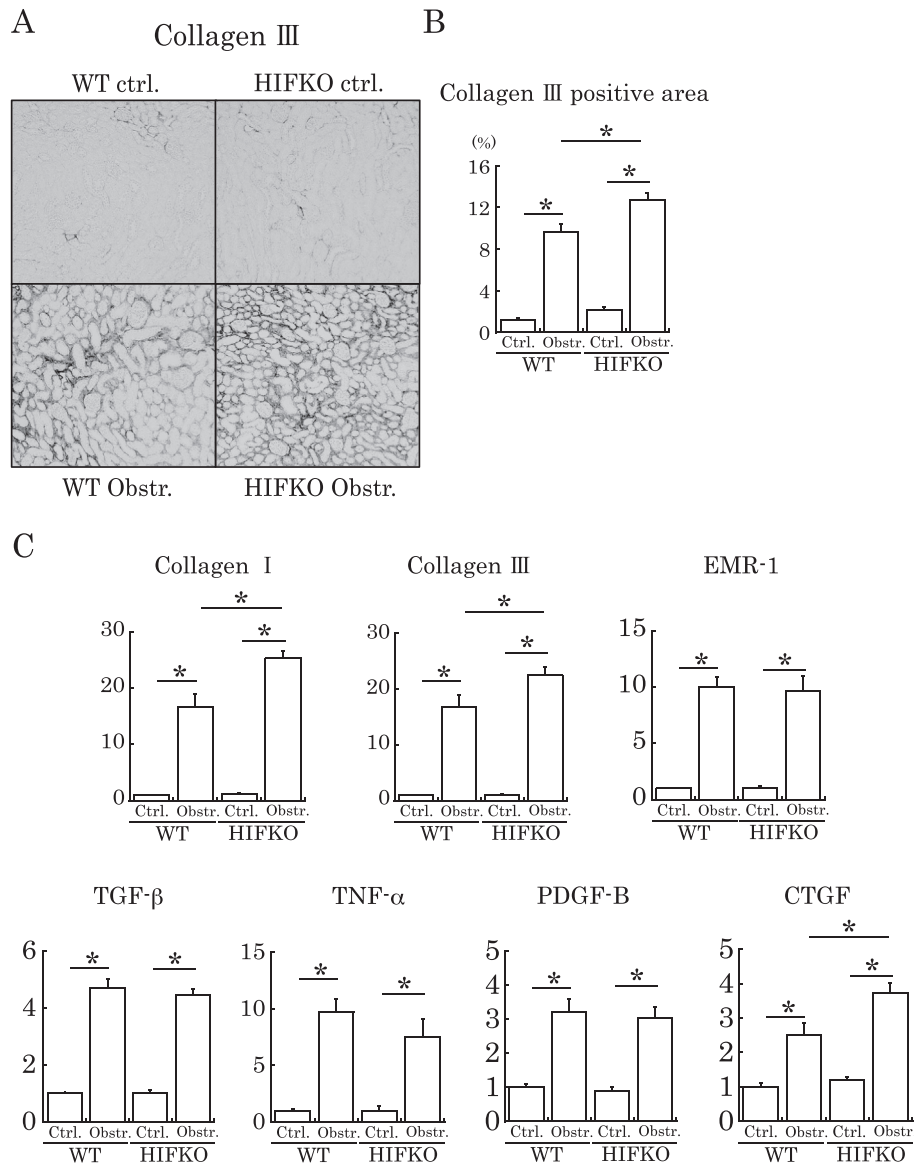


**Fig. 2.** Effects of myeloid HIF-1 depletion on renal fibrosis and renal mRNA expression in obstructed kidneys. A) Representative photographs of renal immunohistochemistry of collagen III depositions at 7 days after UUU (original magnification  $\times 200$ ), and B) percentage of collagen III positive area in the renal cortex were summarized ( $n = 6-7$  in each group). C) Renal mRNA expressions of fibrogenic and proinflammatory molecules in kidney tissues at 7 days after UUU. Each value was corrected for 18S rRNA and mRNA expressions in non-obstructed kidneys of WT group were assigned to a unity ( $n = 6-7$  in each group). Ctrl.: non-obstructed kidneys, Obstr.: obstructed kidneys. \* $p < 0.05$ .

### 3.4. Myeloid HIF-1 depletion did not affect M1 and M2 macrophage phenotype polarization in UUU

There are two macrophage phenotypes, M1 and M2. M1 macrophages express proinflammatory molecules and elicits tissue damage (17). M2 macrophages are involved in wound healing (17). Since HIF-1 expression was enhanced in M1 macrophages but suppressed in M2 macrophages (18), we examined whether myeloid HIF-1 affect the renal macrophage phenotype polarization in the obstructive kidney.

We collected CD11b (+) cells from kidney at 3 and 7 days after UUU by using CD11b MACS beads and evaluated mRNA expressions of M1 and M2 phenotype markers in CD11b (+) cells. The mRNA expression of either M1 markers (TNF- $\alpha$  and IL-1 $\beta$ ) or M2 markers (Arginase-1 and Mrc-1) in CD11b (+) cells obtained from wild type

UUU kidneys was not significantly different from those obtained from HIFKO kidneys (Fig. 4).

Fujiu has shown that F4/80<sup>low</sup> and F4/80<sup>high</sup> macrophages had M1 and M2 phenotypic characteristics respectively (19). Alternatively, Ly6C<sup>high</sup> kidney macrophage exhibited M1-biased pattern of gene expression whereas Ly6C<sup>low</sup> macrophages expressed M2-biased cytokines (11). Therefore, we also tried to distinguish relative population of M1 and M2 polarized macrophages by the intensity of F4/80 and Ly6C expression in the macrophage fraction (Fig. 5A). The cell numbers of either F4/80<sup>low</sup> (F1) or F4/80<sup>high</sup> (F2) macrophages were not different between WT and HIFKO. Similarly, no differences in cell numbers of Ly6C<sup>high</sup> (L1) and Ly6C<sup>low</sup> (L2) macrophages were observed at either 3 days or 7 days after UUU (Fig. 5B, C).

These data suggest that myeloid HIF-1 depletion did not affect M1 and M2 phenotype polarization in UUU.

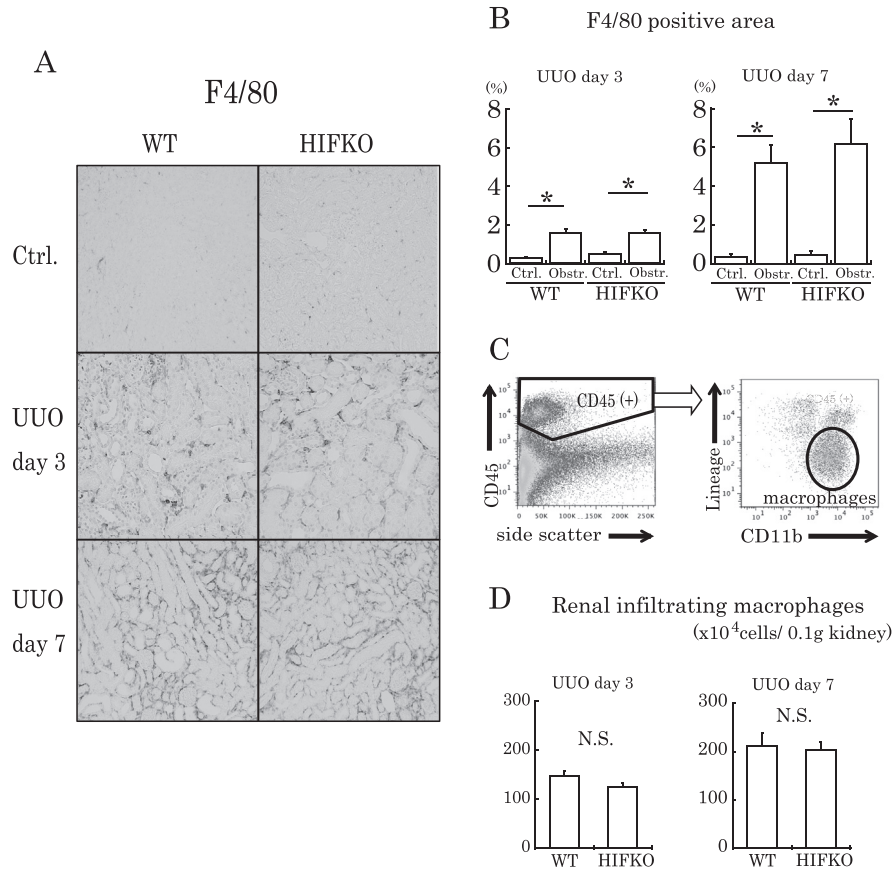


**Fig. 3.** The evaluation of renal infiltrating macrophages at 3 and 7 days after UUO. A) Representative photographs of renal immunohistochemistry of F4/80 (+) cells in the renal cortex at 3 and 7 days after UUO (original magnification  $\times 200$ ), and B) quantitative evaluation of F4/80 (+) cells ( $n = 5-7$  in each group). C) Example of multicolor flow cytometric dot plots and gating used to analyze proportion of individual CD45 (+) cell populations within total renal single cell suspensions from the obstructed kidney (left). CD45 (+) cells were separated by CD11b and Lineage (including anti-CD90.2, B220, NK1.1, CD49b, Ly6G antibodies as markers of leukocytes except for monocytes/macrophages and dendritic cells) (right). Renal infiltrating macrophages were defined as CD45 (+), Lineage (-), CD11b (+) cells. D) The total number of renal infiltrating macrophages (CD45 (+), Lineage (-), CD11b (+) cells) at 3 and 7 days after UUO was determined by flow cytometry ( $n = 4$  in each group). \* $p < 0.05$ . N.S.: not significant.

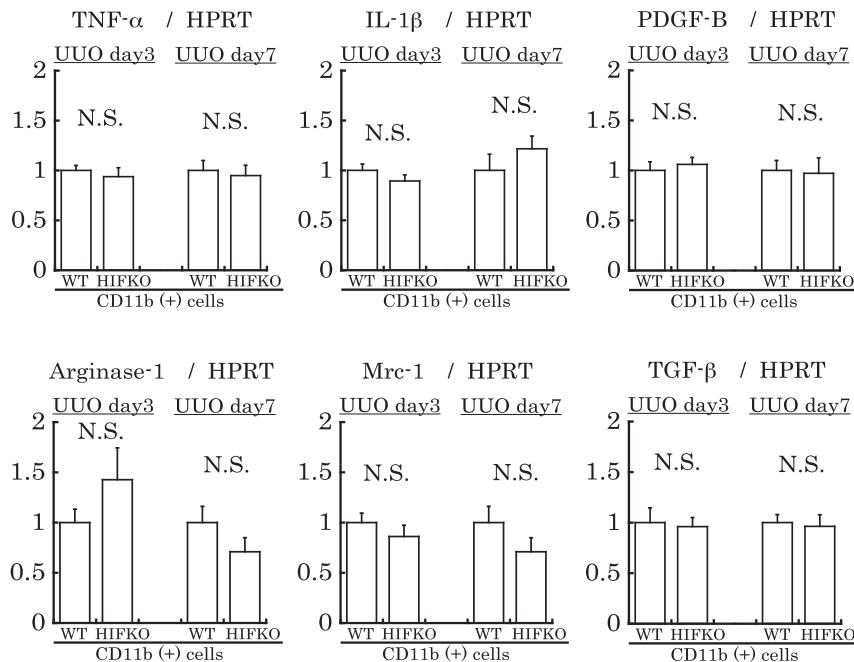


**Fig. 4.** Relative ratio of mRNA expressions of M1 and M2 macrophage phenotype markers and profibrotic molecules in renal CD11b (+) cells of the obstructed kidney. mRNA expressions of WT CD11b (+) cells were assigned to a unity ( $n = 4-8$  in each group). N.S.: not significant.



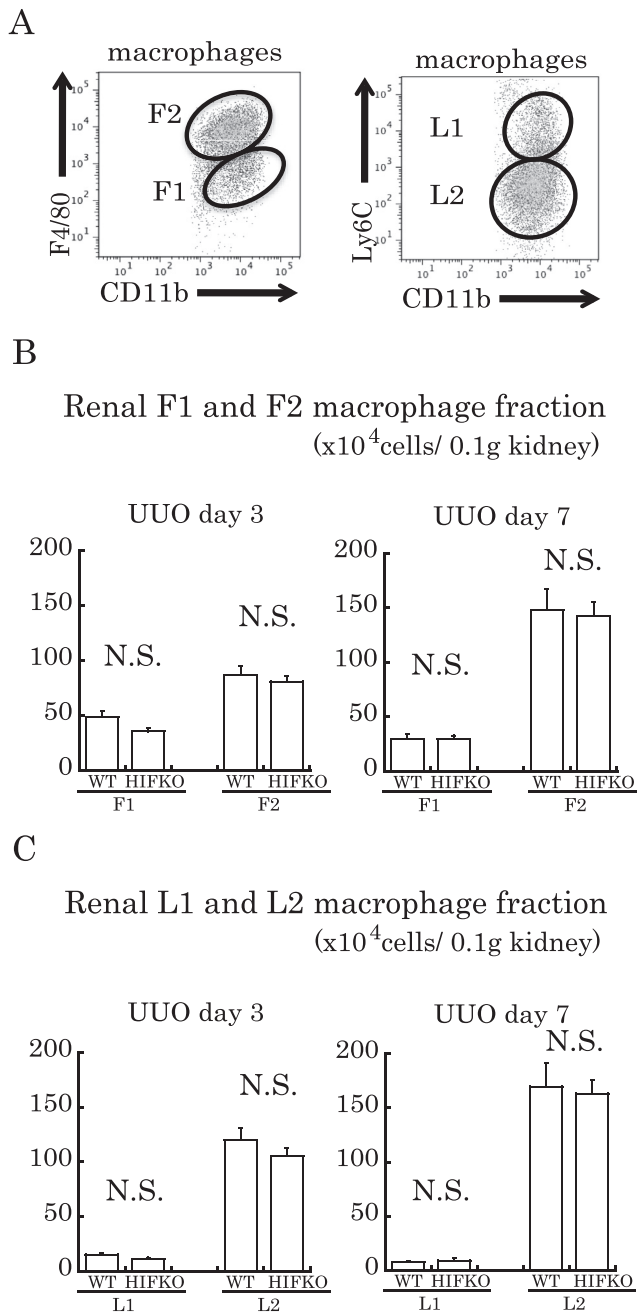


**Fig. 5.** Flow cytometric analysis of relative population of M1 and M2 polarized macrophages classified by the intensity of F4/80 and Ly6C expression. A) Flow cytometric dot plot of renal infiltrating macrophages. Macrophages could be separated into F4/80<sup>low</sup> (F1) and F4/80<sup>high</sup> (F2) fraction that presumably corresponded to M1 and M2 macrophages, respectively (19) (left). Macrophages could be also separated into Ly6C<sup>high</sup> (L1) and Ly6C<sup>low</sup> (L2) fraction that presumably corresponded to M1 and M2 macrophage, respectively (11) (right). B) Cell number of F1 and F2 fraction and C) L1 and L2 fraction of renal infiltrating macrophages at 3 and 7 days after UUO (n = 4 in each group). N.S.: not significant.

### 3.5. Myeloid HIF-1 depletion did not prevent renal tubular injury and apoptotic cell accumulation

Macrophages are closely involved in renal tubular damage (9, 20, 21) and renal epithelial injury triggers interstitial fibrosis (22). Therefore, we tested whether HIF-1 depletion in macrophages affect the tubular injury and apoptosis. The injury of tubular epithelial cells was markedly increased by UUO but myeloid HIF-1

depletion did not affect it (Fig. 6A, C). The cell number of apoptotic tubular cells was also increased by UUO but there were no differences between WT and HIFKO group (Fig. 6B, D). Although TNF- $\alpha$  mediates tubular apoptosis in the obstructed kidney (23, 24), genetic ablation of myeloid HIF-1 did not affect the increased expression of TNF- $\alpha$  mRNA in the obstructed kidney (Fig. 2C). These results indicate that macrophage HIF-1 depletion did not affect renal tubular injury and tubular apoptosis.

### 3.6. Myeloid HIF-1 ablation promoted obstruction-induced increase in CTGF expression

Next, we examined renal mRNA expression of profibrotic molecules in the obstructed kidney. TGF- $\beta$  is a key mediator in the pathogenesis of renal fibrosis (25). TNF- $\alpha$  and platelet-derived growth factor-B (PDGF-B) also mediates the progression of renal fibrosis in murine obstructive nephropathy (26–28). Renal TGF- $\beta$ , TNF- $\alpha$  and PDGF-B mRNA expression was markedly increased by UUO but there were no significant differences between WT and HIFKO group (Fig. 2C). It was also found that TGF- $\beta$  and TNF- $\alpha$  mRNA expression in CD11b (+) cells was significantly higher than that in CD11b (-) cells (Fig. 7C). PDGF-B mRNA expression in CD11b (+) cells was not higher than that in CD11b (-) cells (Fig. 7C). When we compared TGF- $\beta$ , TNF- $\alpha$  and PDGF-B mRNA expression in renal CD11b (+) cell fraction obtained from obstructed kidneys, no significant differences were found between WT and HIFKO group (Fig. 4). We next examined renal CTGF mRNA expression as CTGF plays a pivotal role in the progression of renal fibrosis during UUO (29). Although renal CTGF mRNA expression was increased by UUO, myeloid HIF-1 depletion further enhanced renal CTGF mRNA expression (Fig. 2C). Renal CTGF protein expression in the obstructed kidney was also significantly higher in HIFKO group than WT group (Fig. 7A, B). To examine the source of CTGF, we evaluated CTGF mRNA expression in CD11b (+) cells and CD11b (-) cells. As shown in Fig. 7C, CD11b (-) cells were the predominant source of CTGF mRNA expression. Therefore, these results suggest that macrophage HIF-1 depletion promoted CTGF expression in renal cells other than renal infiltrating macrophages.

## 4. Discussion

The present study showed that specific depletion of myeloid HIF-1, most likely of macrophages, accelerated renal fibrosis in the obstructive nephropathy. Although we and others reported that renal macrophages were involved in the tubular injury and renal fibrogenesis utilizing same animal model (9, 20, 21), our results clearly showed that HIF-1 in macrophages acted to attenuate renal fibrosis.

In our present study, myeloid HIF-1 depletion did not affect the renal accumulation of macrophages or tubular epithelial cell injury observed in the obstructed kidney. Thus, it is unlikely that the accelerated renal fibrosis observed in myeloid HIF-1 KO mouse was either due to enhanced macrophage influx or the increased tissue injurious macrophages. This notion was further supported by the findings that depletion of HIF-1 in macrophages did not affect renal M1 and M2 macrophage phenotype polarization in the obstructed kidney. M1 macrophages are proinflammatory and elicit tissue damage (17, 30). The gene expression analysis of macrophages obtained from obstructed kidneys revealed that mRNA expression of proinflammatory cytokine such as TNF- $\alpha$  and IL-1 $\beta$  were not affected by the macrophage HIF-1 depletion. These findings further support our notion. Our results do not appear to agree with the recent report that genetic ablation of myeloid HIFs markedly stimulated renal macrophage influx but did not affect renal fibrosis in murine obstructive nephropathy (15). Since both HIF-1 and HIF-2

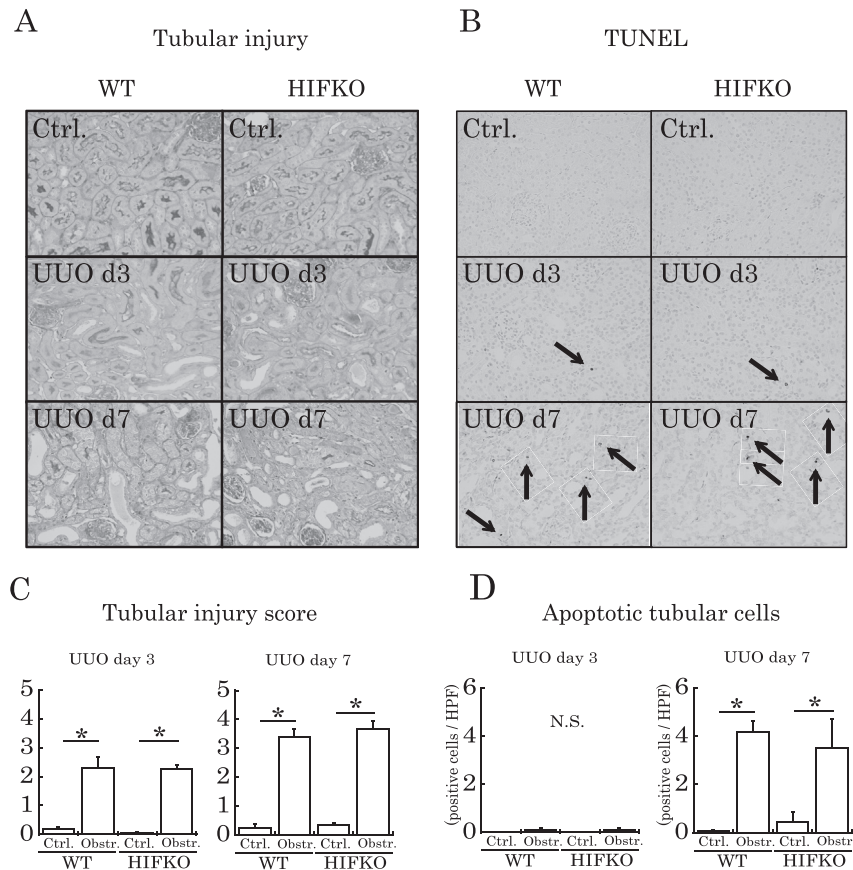


**Fig. 6.** Effects of myeloid HIF-1 depletion on renal tubular injury and apoptotic tubular cells. A) Representative photographs of renal Periodic acid-Schiff (PAS) staining for evaluation of tubular injury and B) renal TUNEL assay for evaluation of renal tubular apoptotic cells at 3 and 7 days after UUO (original magnification  $\times 200$ ). C) Tubular injury scores at 3 and 7 days after UUO (n = 6–7 in each group). D) Quantitative evaluation of TUNEL (+) tubular cells (n = 4 in each group). Arrows indicate apoptotic tubular cells. Ctrl.: non-obstructed kidneys, UUO d3, d7: obstructed kidneys at 3 and 7 days after UUO. \*p < 0.05. N.S.: not significant.

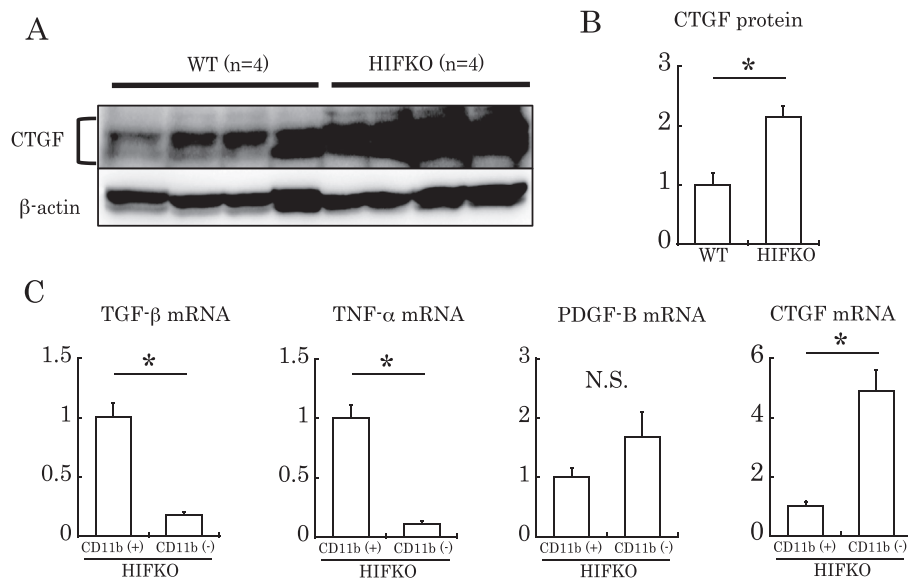


**Fig. 7.** CTGF protein expression in the obstructed kidney and mRNA expression of profibrotic molecules in renal cell fractions. A) Immunoblotting of CTGF proteins in obstructive kidneys of WT and HIFKO mice at 7 days after UUO. (n = 4 in each group), and B) Quantitative evaluation of A). Each value was corrected for  $\beta$ -actin and CTGF protein expression in WT kidney was assigned to a unity. C) mRNA expression of profibrotic molecules in renal CD11b (+) cells and CD11b (-) cells which were separated by CD11b MACS beads at 7 days after UUO. Each value was corrected for 18SrRNA and mRNA expression in CD11b (+) cells was assigned to a unity. (n = 6 in each group), \*p < 0.05.

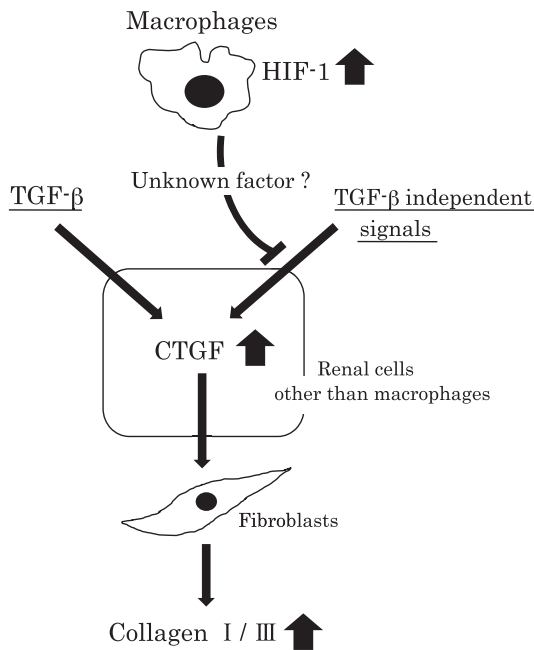


**Fig. 8.** Schematic diagram illustrates the possible mechanisms by which myeloid HIF-1 attenuates the progression of renal fibrosis in the obstructed kidney.

were simultaneously ablated in their study, different results might be explained by the effects of myeloid HIF-2. Future study using mice with genetic ablation of HIF-2 would clarify the role of myeloid HIF-2 itself.

While our present study showed that HIF-1 depletion in macrophages promoted renal fibrosis, myeloid HIF-1 depletion attenuated liver fibrosis in cholestatic mice without affecting tissue injury (31). They suggested that HIF-1 dependent PDGF-B production in macrophages is involved in the mechanisms. In our study, PDGF-B mRNA expression in renal CD11b (+) macrophages was almost the same between WT and HIFKO group. Although the contribution of myeloid HIF-1 to tissue fibrosis varies considerably with the causes and/or organs, HIF-1 in myeloid cells plays a pivotal role in the tissue fibrogenesis.

Although it is difficult to clarify the mechanisms by which myeloid HIF-1 depletion accelerated renal fibrosis, it should be pointed out that ureteral obstruction stimulated mRNA expression of CTGF and myeloid HIF-1 depletion further enhanced it. Renal CTGF protein expression was also stimulated in the obstructed kidney of mice with myeloid HIF-1 depletion. Yokoi et al. reported that CTGF antisense treatment markedly attenuated the induction of CTGF and extracellular matrix genes and reduced renal fibrotic area in rat obstructive nephropathy (29). CTGF is involved in the progression of renal fibrosis in remnant kidney (32) and also diabetic nephropathy (33, 34). Taken together, enhanced CTGF production observed in the obstructed kidney would be one of possible mechanisms by which myeloid HIF-1 depletion promoted renal fibrosis. It was reported that hypoxic induction of CTGF gene expression is directly mediated by HIF-1 (35). If it were the case, ablation of myeloid HIF-1 would have attenuated CTGF gene expression. However, in our study, ablation of myeloid HIF-1 promoted CTGF mRNA and protein expression in the obstructed kidney. This apparent discrepancy can be explained by our finding that CTGF gene expression in the obstructed kidney was mostly derived from renal cells other than CD11b (+) macrophages. In fact, in situ hybridization analysis revealed that upregulation of CTGF mRNA was observed in the myofibroblasts as well as in tubular epithelial

cells in rat obstructive nephropathy (36). Thus, it is conceivable that the presence of HIF-1 in the infiltrating macrophages acted to regulate CTGF expression in the fibroblasts and/or tubular cells of the obstructed kidney. HIF-1 dependent macrophage factors that affected CTGF expression of the obstructed kidney remains to be elucidated. Schematic diagram of this mechanism is shown in Fig. 8.

In the present study, we showed macrophage HIF-1 is protective in renal fibrogenesis as myeloid HIF-1 depletion promoted renal fibrosis. Such anti-fibrotic roles of macrophage HIF-1 is in marked contrast to the profibrotic role of renal tubular HIF-1 as selective depletion of HIF-1 $\alpha$  attenuated renal fibrosis in murine obstructive nephropathy (7). Pharmacological activation of HIF protein by PHD inhibition attenuated interstitial fibrosis in remnant kidneys (6, 37). The PHD inhibitor, GSK1002083A inhibited fibrosis with acute kidney injury (38). Global activation of HIFs with inducible conditional pVHL gene ablation attenuated renal fibrosis of the obstructed kidney (15). These reports suggest that global activation of HIFs is protective in the development of renal fibrosis. In contrast, it was reported that silencing of HIF-1 by small hairpin RNA attenuated renal fibrosis in angiotensin II induced renal injury (39) and in two kidney, one clip chronic ischemic renal injury model (40). These reports suggest the detrimental effect of HIF-1 in the progression of renal fibrosis. Thus, in order to elucidate the role of HIFs in renal fibrogenesis, clarification of relative contribution of individual HIF isoform in specific cell-type should be performed. In this context, it is interesting that PHD inhibition protects against radiation-induced gastrointestinal toxicity exclusively via HIF-2 (41).

Hypoxia-inducible factors have been regarded as a target for drug development. Orally active PHD inhibitor stimulated erythropoietin production in patients with end-stage renal disease (42). Efforts are underway to identify inhibitor of HIF-1 activity for cancer therapy. Clarification of individual HIF isoform in specific cell-type would provide valuable information to anticipate the efficacy and adverse effects of drugs that target HIF.

### Conflict of interest

All authors declare no conflict of interest.

### Acknowledgments

This work was supported by JSPS KAKENHI Grant Number 25460656 and a grant from the Osaka Kidney Foundation.

### References

- (1) Liu Y. Renal fibrosis: new insights into the pathogenesis and therapeutics. *Kidney Int.* 2006;69:213–217.
- (2) Nangaku M, Fujita T. Activation of the renin-angiotensin system and chronic hypoxia of the kidney. *Hypertens Res.* 2008;31:175–184.
- (3) Schofield CJ, Ratcliffe PJ. Oxygen sensing by HIF hydroxylases. *Nat Rev Mol Cell Biol.* 2004;5:343–354.
- (4) Nangaku M, Eckardt KU. Hypoxia and the HIF system in kidney disease. *J Mol Med Berl.* 2007;85:1325–1330.
- (5) Matsumoto M, Makino Y, Tanaka T, Tanaka H, Ishizaka N, Noiri E, et al. Induction of renoprotective gene expression by cobalt ameliorates ischemic injury of the kidney in rats. *J Am Soc Nephrol.* 2003;14:1825–1832.
- (6) Song YR, You SJ, Lee YM, Chin HJ, Chae DW, Oh YK, et al. Activation of hypoxia-inducible factor attenuates renal injury in rat remnant kidney. *Nephrol Dial Transpl.* 2010;25:77–85.
- (7) Higgins DF, Kimura K, Bernhardt WM, Shrimanker N, Akai Y, Hohenstein B, et al. Hypoxia promotes fibrogenesis in vivo via HIF-1 stimulation of epithelial-to-mesenchymal transition. *J Clin Invest.* 2007;117:3810–3820.
- (8) Kimura K, Iwano M, Higgins DF, Yamaguchi Y, Nakatani K, Harada K, et al. Stable expression of HIF-1 $\alpha$  in tubular epithelial cells promotes interstitial fibrosis. *Am J Physiol Renal Physiol.* 2008;295:F1023–F1029.
- (9) Kitamoto K, Machida Y, Uchida J, Izumi Y, Shiota M, Nakao T, et al. Effects of liposome clodronate on renal leukocyte populations and renal fibrosis in murine obstructive nephropathy. *J Pharmacol Sci.* 2009;111:285–292.



- (10) Machida Y, Kitamoto K, Izumi Y, Shiota M, Uchida J, Kira Y, et al. Renal fibrosis in murine obstructive nephropathy is attenuated by depletion of monocyte lineage, not dendritic cells. *J Pharmacol Sci.* 2010;114:464–473.
- (11) Lin SL, Castano AP, Nowlin BT, Lupher Jr ML, Duffield JS. Bone marrow Ly6Chigh monocytes are selectively recruited to injured kidney and differentiate into functionally distinct populations. *J Immunol.* 2009;183:6733–6743.
- (12) Anand RJ, Gribar SC, Li J, Kohler JW, Branca MF, Dubowski T, et al. Hypoxia causes an increase in phagocytosis by macrophages in a HIF-1alpha-dependent manner. *J Leukoc Biol.* 2007;82:1257–1265.
- (13) Fujisaka S, Usui I, Ikutani M, Aminuddin A, Takikawa A, Tsuneyama K, et al. Adipose tissue hypoxia induces inflammatory M1 polarity of macrophages in an HIF-1alpha-dependent and HIF-1alpha-independent manner in obese mice. *Diabetologia.* 2013;56:1403–1412.
- (14) Nakayama T, Kurobe H, Sugawara N, Kinoshita H, Higashida M, Matsuoka Y, et al. Role of macrophage-derived hypoxia-inducible factor (HIF)-1alpha as a mediator of vascular remodelling. *Cardiovasc Res.* 2013;99:705–715.
- (15) Kobayashi H, Gilbert V, Liu Q, Kapitsinou PP, Unger TL, Rha J, et al. Myeloid cell-derived hypoxia-inducible factor attenuates inflammation in unilateral ureteral obstruction-induced kidney injury. *J Immunol.* 2012;188:5106–5115.
- (16) Swirski FK, Nahrendorf M, Etzrodt M, Wildgruber M, Cortez-Retamozo V, Panizzi P, et al. Identification of splenic reservoir monocytes and their deployment to inflammatory sites. *Science.* 2009;325:612–616.
- (17) Ferrante CJ, Leibovich SJ. Regulation of macrophage polarization and wound healing. *Adv Wound Care (New Rochelle).* 2012;1:10–16.
- (18) Takeda N, O'Dea EL, Doedens A, Kim JW, Weidemann A, Stockmann C, et al. Differential activation and antagonistic function of HIF-1alpha isoforms in macrophages are essential for NO homeostasis. *Genes Dev.* 2010;24:491–501.
- (19) Fujii K, Manabe I, Nagai R. Renal collecting duct epithelial cells regulate inflammation in tubulointerstitial damage in mice. *J Clin Invest.* 2011;121:3425–3441.
- (20) Duffield JS, Tipping PG, Kipari T, Cailhier JF, Clay S, Lang R, et al. Conditional ablation of macrophages halts progression of crescentic glomerulonephritis. *Am J Pathol.* 2005;167:1207–1219.
- (21) Sean Eardley K, Cockwell P. Macrophages and progressive tubulointerstitial disease. *Kidney Int.* 2005;68:437–455.
- (22) Grgic I, Campanholle G, Bijol V, Wang C, Sabbiseti VS, Ichimura T, et al. Targeted proximal tubule injury triggers interstitial fibrosis and glomerulosclerosis. *Kidney Int.* 2012;82:172–183.
- (23) Misseri R, Meldrum DR, Dinarello CA, Dagher P, Hile KL, Rink RC, et al. TNF-alpha mediates obstruction-induced renal tubular cell apoptosis and proapoptotic signaling. *Am J Physiol Ren Physiol.* 2005;288:F406–F411.
- (24) Meldrum KK, Metcalfe P, Leslie JA, Misseri R, Hile KL, Meldrum DR. TNF-alpha neutralization decreases nuclear factor-kappaB activation and apoptosis during renal obstruction. *J Surg Res.* 2006;131:182–188.
- (25) Yanagita M. Inhibitors/antagonists of TGF-beta system in kidney fibrosis. *Nephrol Dial Transplant.* 2012;27:3686–3691.
- (26) Guo G, Morrissey J, McCracken R, Tolley T, Klahr S. Role of TNFR1 and TNFR2 receptors in tubulointerstitial fibrosis of obstructive nephropathy. *Am J Physiol.* 1999;277:F766–F772.
- (27) Meldrum KK, Misseri R, Metcalfe P, Dinarello CA, Hile KL, Meldrum DR. TNF-alpha neutralization ameliorates obstruction-induced renal fibrosis and dysfunction. *Am J Physiol Regul Integr Comp Physiol.* 2007;292:R1456–R1464.
- (28) Lin SL, Chang FC, Schrimpf C, Chen YT, Wu CF, Wu VC, et al. Targeting endothelium-pericyte cross talk by inhibiting VEGF receptor signaling attenuates kidney microvascular rarefaction and fibrosis. *Am J Pathol.* 2011;178:911–923.
- (29) Yokoi H, Mukoyama M, Nagae T, Mori K, Suganami T, Sawai K, et al. Reduction in connective tissue growth factor by antisense treatment ameliorates renal tubulointerstitial fibrosis. *J Am Soc Nephrol.* 2004;15:1430–1440.
- (30) Sica A, Mantovani A. Macrophage plasticity and polarization: in vivo veritas. *J Clin Invest.* 2012;122:787–795.
- (31) Copple BL, Kaska S, Wentling C. Hypoxia-inducible factor activation in myeloid cells contributes to the development of liver fibrosis in cholestatic mice. *J Pharmacol Exp Ther.* 2012;341:307–316.
- (32) Okada H, Kikuta T, Kobayashi T, Inoue T, Kanno Y, Takigawa M, et al. Connective tissue growth factor expressed in tubular epithelium plays a pivotal role in renal fibrogenesis. *J Am Soc Nephrol.* 2005;16:133–143.
- (33) Ito Y, Aten J, Bende RJ, Oemar BS, Rabelink TJ, Weening JJ, et al. Expression of connective tissue growth factor in human renal fibrosis. *Kidney Int.* 1998;53:853–861.
- (34) Wahab NA, Yevdokimova N, Weston BS, Roberts T, Li XJ, Brinkman H, et al. Role of connective tissue growth factor in the pathogenesis of diabetic nephropathy. *Biochem J.* 2001;359:77–87.
- (35) Higgins DF, Biju MP, Akai Y, Wutz A, Johnson RS, Haase VH. Hypoxic induction of Ctgf is directly mediated by Hif-1. *Am J Physiol Ren Physiol.* 2004;287:F1223–F1232.
- (36) Yokoi H, Mukoyama M, Sugawara A, Mori K, Nagae T, Makino H, et al. Role of connective tissue growth factor in fibronectin expression and tubulointerstitial fibrosis. *Am J Physiol Ren Physiol.* 2002;282:F933–F942.
- (37) Tanaka T, Kojima I, Ohse T, Ingelfinger JR, Adler S, Fujita T, et al. Cobalt promotes angiogenesis via hypoxia-inducible factor and protects tubulointerstitium in the remnant kidney model. *Lab Invest.* 2005;85:1292–1307.
- (38) Kapitsinou PP, Jaffe J, Michael M, Swan CE, Duffy KJ, Erickson-Miller CL, et al. Preischemic targeting of HIF prolyl hydroxylation inhibits fibrosis associated with acute kidney injury. *Am J Physiol Ren Physiol.* 2012;302:F1172–F1179.
- (39) Zhu Q, Wang Z, Xia M, Li PL, Van Tassel BW, Abbate A, et al. Silencing of hypoxia-inducible factor-1alpha gene attenuates angiotensin II-induced renal injury in Sprague-Dawley rats. *Hypertension.* 2011;58:657–664.
- (40) Wang Z, Zhu Q, Li PL, Dhaduk R, Zhang F, Gehr TW, et al. Silencing of hypoxia-inducible factor-1alpha gene attenuates chronic ischemic renal injury in two-kidney, one-clip rats. *Am J Physiol Ren Physiol.* 2014;306:F1236–F1242.
- (41) Taniguchi CM, Miao YR, Diep AN, Wu C, Rankin EB, Atwood TF, et al. PHD inhibition mitigates and protects against radiation-induced gastrointestinal toxicity via HIF2. *Sci Transl Med.* 2014;6:236–264.
- (42) Bernhardt WM, Wiesener MS, Scigalla P, Chou J, Schmieder RE, Gunzler V, et al. Inhibition of prolyl hydroxylases increases erythropoietin production in ESRD. *J Am Soc Nephrol.* 2010;21:2151–2156.